Supplementary Information (SI) for Environmental Science: Nano.
This journal is © The Royal Society of Chemistry 2025

Cyanobacteria-derived biochar supported ZIF-8 derived ZnS-NC for superior peroxymonosulfate activation to removal 4-chlorophenol from wastewater

Ronghan Wang [a, 1], Qingkai Shi [a, 1], Wenjun Wang [b], Guangfu Wang [a], Yang Liu [c], Jun Wang [c], Chengyun Zhou [a], Min Cheng [a, *], Weiping Xiong [a, *], Dongbo Wang [a, *]

[a] College of Environmental Science and Engineering, Key Laboratory of Environmental Biology and Pollution Control (Ministry of Education), Hunan University, Changsha 410082, China

[b] School of Resources and Environment, Hunan University of Technology and Business, Changsha 410205, PR China

[c] School of Minerals Processing and Bioengineering, Key Laboratory of Biohydrometallurgy of Ministry of Education, Central South University, Changsha 410083, China

---

[1] These authors contribute equally to this article.

[*] Corresponding authors. College of Environmental Science and Engineering, Hunan University, Changsha, Hunan 410082, China.

E-mail address: chengmin@hnu.edu.cn (M. Cheng), xiongweiping@hnu.edu.cn (W. Xiong), dongbowang@hnu.edu.cn (D. Wang).

Text S1. Chemical and agents

Zinc nitrate ($Zn(NO_3)_2·6H_2O$), sublimated sulfur (S), sodium thiosulfate ($Na_2S_2O_3$), methyl alcohol (MeOH), ethanol (EtOH), sulfuric acid (H_2SO_4), sodium hydroxide (NaOH), sodium chloride (NaCl), sodium sulfate (Na_2SO_4), sodium bicarbonate (Na_2CO_3), *tert*-butanol (TBA), L-histidine (L-his) were obtained from Sinopharm Chemical Reagent Co., Ltd. 2-methylimidazole (2-MeIM) and 4-chlorophenol (4-CP) were supplied by Macklin Biochemical Co. Ltd. (Shanghai, China). Oxidant ($KHSO_5·0.5KHSO_4·0.5K_2SO_4$, PMS), tetrachloroethylene (CCl_4), *p*-benzoquinone (*p*-BQ), and humic acid (HA) were obtained from Shanghai Rhawn Chemical reagent Co., Ltd. (Shanghai China).

Text S2. Materials synthesis

Biochar (BC) was obtained by the pyrolysis of 20 g *cyanobacteria* biomass that collected from the Taihu Lake, China in 400 °C for 2 h at a heating rate of 5 °C/min under N_2 atmosphere. Before entering the tube furnace, the biomass was thoroughly dried under 80 °C and crushed into particles below 100 mesh to enable adequate pyrolysis.

To synthesize ZIF-8/BC-1, ZIF-8 was uniformly dispersed on the BC substrate through in-situ nucleation and growth. Firstly, 1 g of BC and 1.19 g of $Zn(NO_3)_2·6H_2O$ were dispersed in 30 mL methanol (MeOH) by ultrasound to obtain solution A. Solution B was obtained by dissolving 1.314 g of 2-MIM into a 15 mL MeOH solution by stirring. Subsequently, solution A was quickly poured into solution B and continued vigorously stirring for 1 h. The mixed solution was then transferred into a 100 mL polytetrafluoroethylene reactor and maintained at 120 ℃ for 4 h. ZIF-8/BC-1 was separated by vacuum filtration and cleaned three times with MeOH and N,N-Dimethylformamide (DMF), respectively. Finally, the prepared material was vacuum dried at 60 ℃ for 12 h and ground to powder. ZIF-8 was synthesized in the absence of BC, while several ZnS-NC/BC-x were synthesized (x represented the quality of BC during the synthesis of ZIF-8 and BC composite, including 0.5 g, 1 g, 1.5 g, and 2 g). Dispersion of ZIF-8 particles could be sufficiently avoided by loading ZIF-8 onto the supportive BC. As shown in Fig. S1a, most of the ZIF-8 particles were agglomerated together, which would lead to incomplete exposure of the active site. After the introduction of BC substrate, the dispersion of ZIF-8 particles was significantly enhanced (Fig. 1b), which promoted the final material properties.

0.4 g ZIF-8/BC-1 was dispersed in a 20 mL sulfur-containing solution (v(CCl_4)/v (EtOH) = 4/1) and stirred at 60 °C to dry. The collected mixture was then transferred to a quartz ceramic boat and subjected to pyrolysis at 900 °C for 2 h under N_2 conditions, with a heating rate of 5 °C/min. The product after pyrolysis was pickled with 80 mL of 2 M H_2SO_4. Filter and vacuum dry to obtain the final ZnS-NC/BC-1. The step of acid washing was essential. The removal ability of ZnS-NC/BC-1 for 4-CP before and after acid washing was compared. As shown in Fig. S1d, the 4-CP removal efficiency of ZnS-NC/BC-1 after acid washing was significantly higher than that of it before acid washing. It was speculated that during the pyrolysis process, the excess S coated on the surface of material in the form of ZnS through trapping the volatilized Zn, thus blocking the contact of the reactants with the catalyst. From Fig. S1b and c, the surface of ZnS-NC/BC-1 before acid washing was covered, and the surface of the material after acid washing exposes rough sites (Fig. 1c). And from the distribution of elements (Fig. S1e and Fig. 1d), the Zn and S contents were significantly higher before acid washing than after acid washing, which initially confirmed above speculation. It was noteworthy that ZnS particles were undoubtedly exposed in the elemental mapping images, while they disappeared after acid washing, proving that most of the ZnS particles were removed during the pickling process. Besides, the specific surface area and porosity of the materials before and after acid washing were also compared. As shown in Fig. S1f, g and Table S2, the specific surface area and porosity of the materials were significantly enhanced after acid washing, which might be exactly caused by the excess S blocking the pores. Furthermore, XPS was used to further confirm the speculation. The result exhibited (Table S3) a significant decrease in Zn and S content after acid washing. In addition, by comparing the fine high-resolution XPS spectra of N and S (Fig. S1h-i and Table S4), the contents of pyridinic N and thiophene S were significantly improved, which would be potential active sites for superior PMS activation performance.

Text S3. Characteristic methods

Scanning electron microscope (SEM) (Sigma 300, ZEISS, German) was used to determine the morphology of samples. Elemental mapping was measured by energy dispersive X-ray spectroscopy (EDX). The specific surface area (S_{BET}), and pore volume (V_{pore}) and size were measured by N_2-Brunauer-Emmett-Teller (BET, Micromeritics ASAP 2460 3.01). The pore structures of the samples were confirmed by their mesopore size distributions as determined by Barrett-Joyner-Halenda (BJH) methods. The phase composition of the samples was determined through X-ray diffraction (XRD) (Smartlab, Rigaku, Japan) with Cu Kα radiation at a scan speed of 10° min^{-1} in the range of 5° to 90°. Fourier transform infrared (FTIR) was used to obtain chemical groups and bonds. Raman spectra were acquired using a confocal Raman spectrometer with a 532 nm laser as the excitation source (LabRAM HR Evolutio, Horiba, Japan) to characterize the carbon support. The composition and chemical states of the surface elements were obtained by using X-ray photoelectron spectroscopy (XPS) (K-Alpha, Thermo Scientific, USA). The electron paramagnetic resonance (EPR) signal was measured by Bruker EMXplus spectrometer 5,5-dimethyl-1-pyrroline-N-oxide (DMPO) and 2,6,6-Tetramethylpiperidine (TEMP) as the spin-trapping agents. Excitation-emission matrix (EEM) of natural water before and after reaction was measured by F-7000, HITACHI and the substance content corresponding to different regions were obtained by regional points after removing Rayleigh scattering and Raman scattering. The total organic carbon (TOC) was measured with a TOC analyzer (Multi N/C 3100, Jena, German).

Text S4. Degradation experiment and analytical method

In a typical degradation experiment, 50 mL of 10 mg/L 4-CP solution was added to a 100 mL beaker. 0.2 g/L ZnS-NC/BC-1 was added into the beaker and stirred for 1 h to achieve adsorption-desorption equilibrium. During continuous stirring, 0.1 g/L PMS was injected into the solution to initiate the degradation reaction. At the pre-set time points, 1 mL of the sample was taken out and 20 μL of 0.1M $Na_2S_2O_3$ was added to terminate the reaction.

The 4-CP degradation was monitored by a 1260 Infinity HPLC (Agilent, USA) equipped with a UV detector and a Poroshell 120 ECC18 column (4.6 × 100 mm, 2.7 μm). The detection of 4-CP was procced under 280 nm with a mobile phase of 30% H_2O + 70% methyl alcohol.

Text S5. PMS consumption

The PMS consumption was detected colorimetric method. In brief, 0.332 ~ 0.34 g KI and 0.08 g $NaHCO_3$ were dissolved in 200 mL H_2O to prepare KI stock solution. Then, 0.5 mL of reaction solution was added into 4.5 mL of KI stock solution at designated time intervals for reaction 5 min, followed by analyzed on a UV–vis spectrophotometer at 352 nm.

Text S6. Electrochemical Tests

Electrochemical impedance spectroscopy (EIS), and chronoamperometry (I-T) test were carried out on a CHI760E electrochemical workstation with a three-electrode cell to explore the electron transfer process. Here, platinum foil, catalyst-modified glassy carbon and Ag/AgCl electrode were deemed as the counter electrode, working electrode and reference electrode, respectively. Na_2SO_4 solution (0.2 M) aqueous solution was used as the electrolyte. The working electrode was prepared as follows: homogeneous catalyst ink was first prepared by sonication of 5 mg catalyst powder, 0.2 mL Nafion solution (5 wt%, Sigma-Aldrich) and 0.8 mL absolute ethanol. Then, 100 μL of the as-prepared catalyst ink was pipetted onto the surface of the glassy carbon electrode. The catalyst layer was dried in ambient air before use. Under the condition of room temperature, all the electrochemical measurements were obtained without bias potential.

Text S7. Liquid chromatography-mass spectrometry (LC-MS)

The intermediate products produced from the degradation of 4-CP were determined by liquid chromatography-mass spectrometry (LC-MS) to infer the pathway of TC-HCl degradation. In the degradation experiments, samples were taken at 10, 30, and 60 min to determine the by-products and filtrated through a 0.22 μm nylon filter membrane. In this work, solid phase extraction (SPE) method was used to pre-treat the samples to be measured. In each process, the SPE column (60 mg, 3 ml) was first activated with 5 mL of methanol and 5 mL of ultrapure water, and then 5 mL of the sample solution was slowly passed through the SPE column to complete the uploading of the sample. Subsequently, the column was washed with ultrapure water for the removal of interfering substances, and then the sample was eluted with 5 mL of methanol. The degradation intermediates of 4-CP were investigated using an LC-MS system (1290/6460 Triple Quad, Agilent) and a Kromasil C18 column (250 × 4.6 mm, 5 μm). The detailed gradient elution was programmed in Table S1.

Text S8. Toxicity evaluation

Toxicity evaluation of 4-CP and the degradation intermediates was carried out using Toxicity Evaluation Software Tool program (T.E.S.T., V5.1.2). T.E.S.T. can predict the toxicity of different degradation products of 4-CP through quantitative structure activity relationship methodologies. In this work, based on the consensus method, the average predicted toxicity of multiple methods, six types of toxicity were evaluated, including Oral rat 50 percent lethal dose (Oral rat LD_{50}), Ames Mutagenicity, Bioaccumulation factor, 96-hour fathead minnow 50 percent lethal concentration (Fathead minnow LC_{50} (96 h)), 48-hour daphnia magna 50 percent lethal concentration (Daphnia magna LC_{50} (48 h)), and Tetrahymena pyriformis 50 percent growth inhibition concentration (T. pyriformis IGC_{50}).

Text S9. Theoretical calculation

The theoretical calculations were all carried out based on the density functional theory (DFT) in Gaussian 16, in which the B3LYP functional with a 6-31G(d) basis set was used to perform geometric optimization and frequency calculation for 4-CP. Subsequently, single point energy calculation was performed based on the B3LYP functional with a 6-31G(d, p) basis set after optimizing 4-CP. The contribution of Fukui function was conducted by Multiwfn 3.8 and the electrostatic potential on molecular surface was plotted by Multiwfn 3.8, and Visual Molecular Dynamics (VMD).

Text S10. Natural water and sewage effluent

The natural water bodies (River Xiangjiang and Lake Taozi) came from Changsha, China. The sewage effluent was collected from the sewage treatment plant in Changsha, China. Before conducting the experiment, the collected water samples were first left to stand overnight and then filtered to remove insoluble impurities from the water. Table S5 summarized the basic physical and chemical properties of different water samples. Among them, total hardness, total organic carbon, chemical oxygen demand, and metal ion concentration were determined by ethylenediaminetetraacetic acid disodium titration, TOC analyzer, dichromate method, and inductively coupled plasma mass spectrometry (ICP-MS), respectively.

Text S11. Cyclic and continuous experiments

For the evaluation of the reusability of ZnS-NC/BC-1, a cycling experiment was conducted in this study. In order to avoid the impact of catalyst loss on the catalyst changes in each cycle (including losses from sampling, pumping and drying, and grinding, etc.) for more concentration on the catalyst changes, multiple batch experiments were set up in the first cycle. After cycling, the performance of ZnS-NC/BC-1 decreased, thus we resurrected it and performed post-resurrection cycling experiments. The catalyst was regenerated by calcining at 400 °C for 20 min with a heating rate of 5 °C/min under N_2 protection. In each cycle, the reaction conditions remained consistent and one of the breakers was randomly selected for sampling to determine the degradation efficiency of 4-CP.

The packed column technique was used to construct a continuous reactor to further explore its potential for practical applications. The packed columns consisted of cotton, large-particle quartz sand, small-particle quartz sand and nano sponges absorbed with 100 mg of ZnS-NC/BC-1 from both ends towards the middle. A peristaltic pump (0.25 mL/min) was responsible for pumping in PMS (200 mg/L) and 4-CP (10 mg/L), while an automatic collector (15 min/sample) was responsible for collecting the degraded samples. The collected samples were sent to the HPLC for determination.

Text S12. Phytotoxicity test

Pakchoi was used to test the toxic effects of the effluent on seed germination and growth before and after the reaction. 10 mg/L of 4-CP solution and the solution collected after the reaction were used to cultivate seed germination and growth of Pakchoi, and deionized water was used as a control. Specifically, a total of 60 seeds were grown in each group and sterilized with 3% H_2O_2 for 30 min before proceeding with the incubation. On day 0, 5 mL of solution was used to initiate seed germination and subsequently 2 mL of solution would be added daily. The experiment was carried out for 5 days, of which the first two days were under dark conditions, and when the seeds had almost completed germination on day 2, they were transferred to natural light. The germination of the seeds was recorded daily during the experiment. After 5 days, the strength of the toxicity of the different liquids was determined by measuring the rhizome length of the seedlings.

Text S13. Reaction kinetics

The pseudo-first order kinetic model was adopted to study the reaction kinetics.

$$ln\frac{C_0}{C} = k_{obs}t$$

where C_0 ($mg \cdot L^{-1}$) is the initial concentration of TC-HCl, C is the concentration at time t, t represents the time, and k_{obs} (min^{-1}) is the pseudo-first order rate constant.

Text S14. Calculation for the contribution of different ROS.

The kinetic evaluation was further utilized to calculate the contribution rate of different ROS. According to the quenching experiments, although the contribution of •OH and $SO_4^{\bullet -}$ to 4-CP degradation had been largely excluded due to the limited inhibitions, but the reaction kinetic after adding MeOH still decreased from 0.0336 min^{-}

^{1} to 0.0228 min^{-1}, which should be included into the calculation. The reaction rate constant without any quenchers was k_0, and the reaction rate constants after adding p-BQ and L-his, MeOH were denoted as k_1, k_2 and k_3, respectively. The contribution of $O_2^{\bullet -}$, and $^1O_2$ was calculated according to the following equations.

$$\lambda\left(O^{\cdot -}_{2}\right) = \frac{k_0 - k_1}{k_0} \times 100\%$$

$$\lambda(1O2) = \frac{k_0 - k_2}{k_0} \times 100\%$$

$$\lambda\left(\bullet OH + SO^{\bullet -}_{4}\right) = \frac{k_0 - k_3}{k_0} \times 100\%$$

Where $\lambda(O_2^{\bullet -})$, $\lambda(^1O_2)$, and $\lambda(\bullet OH+SO_4^{\bullet -})$ represented the contribution rate of $O_2^{\bullet -}$, $^1O_2$, and $\bullet OH+SO_4^{\bullet -}$ respectively. Subsequently, the calculated values were harmonized and standardized.

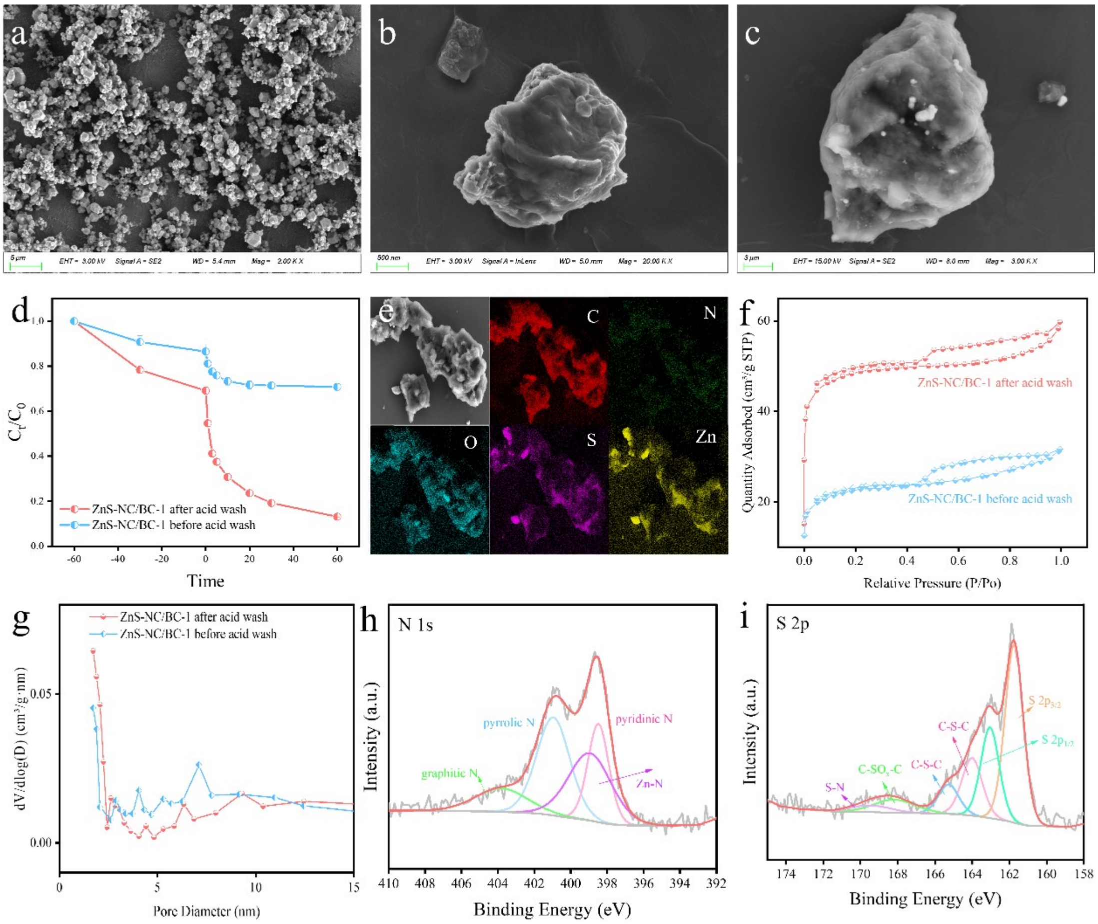

Fig. S1. SEM images of (a) agglomerated ZIF-8 particles, (b-c) ZnS-NC/BC-1 before acid washing. (d) The 4-CP removal efficiency of ZnS-NC/BC-1 before and after acid washing. (e) EDS elemental mappings images of ZnS-NC/BC-1 before acid washing. (f) N_2 adsorption-desorption isotherms and (g) Pore size distribution plots of ZnS-NC/BC-1 before and after acid washing. High-resolution XPS spectra of (h) N 1s and (i) S 2p, respectively.

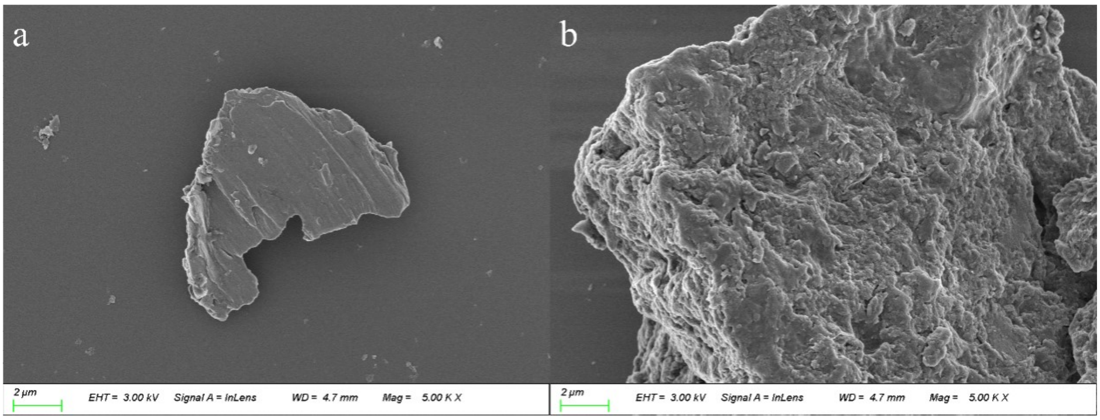

Fig. S2. SEM images of BC with (a) smooth and (b) rough surfaces.

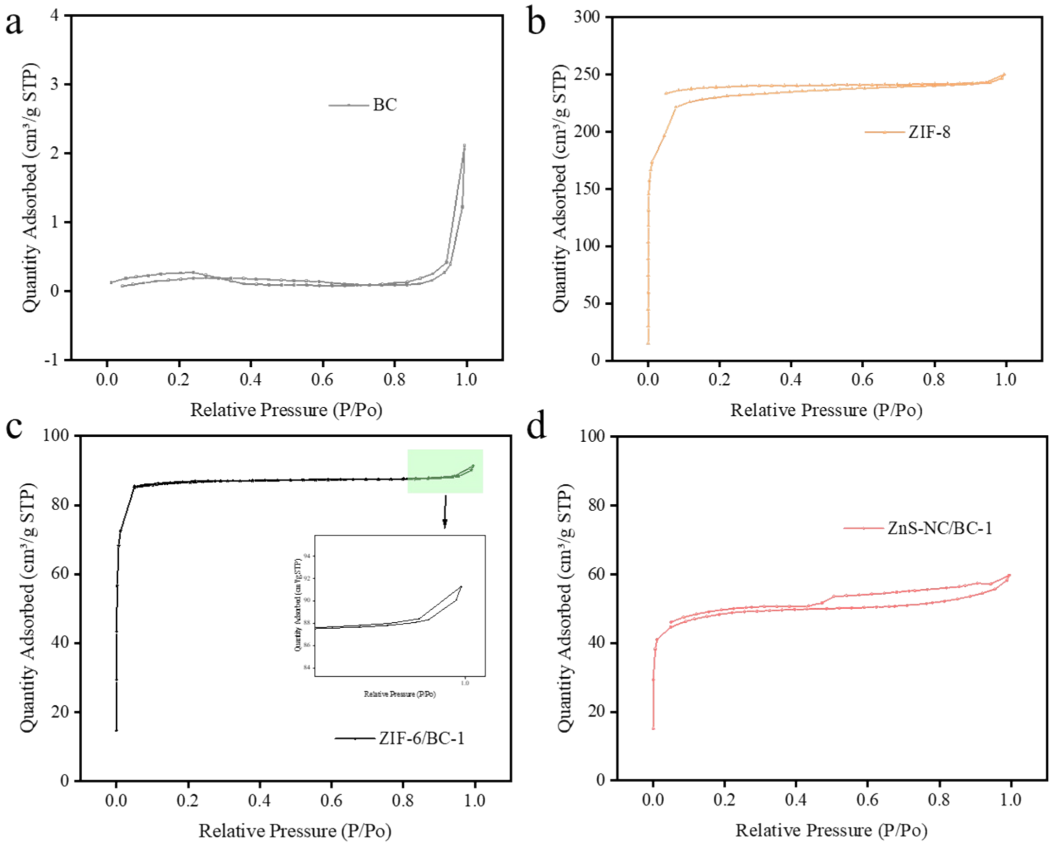

Fig. S3. N_2 adsorption-desorption isotherms of (a) BC, (b) ZIF-8, (c) ZIF-8/BC-1, and (d) ZnS-NC/BC-1.0.

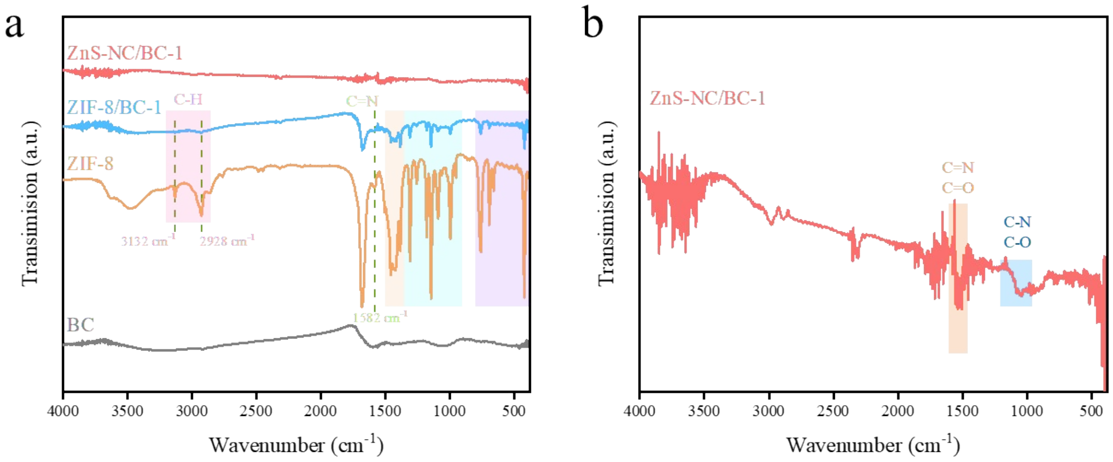

Fig. S4. (a) FTIR spectra of BC, ZIF-8, ZIF-8/BC-1, and ZnS-NC/BC-1. (b) The magnified FTIR pattern of ZnS-NC/BC-1.

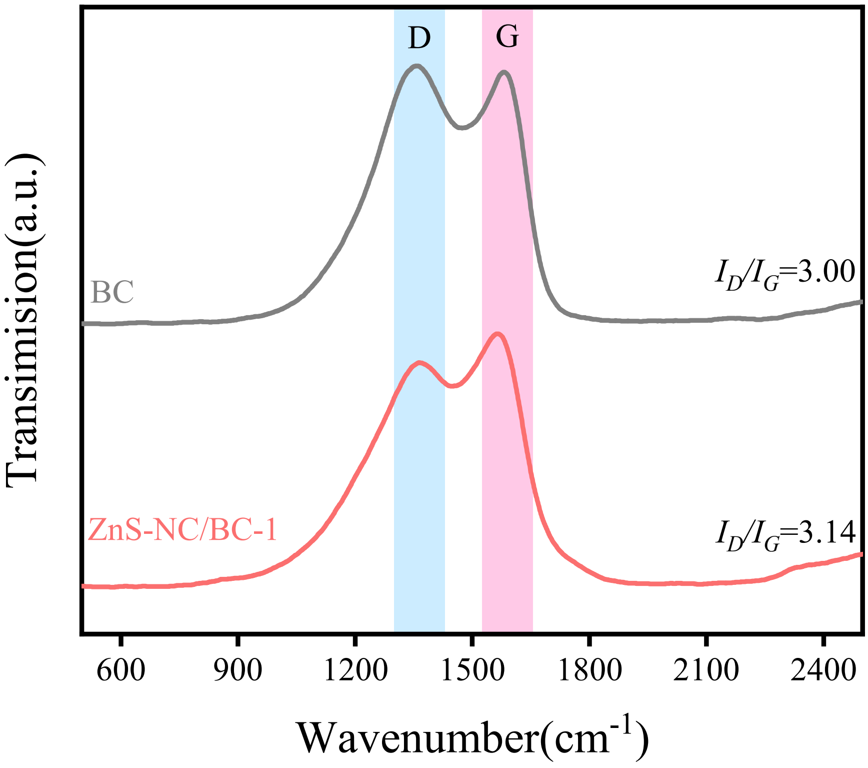

Fig. S5. Raman spectra of BC, and ZnS-NC/BC-1.

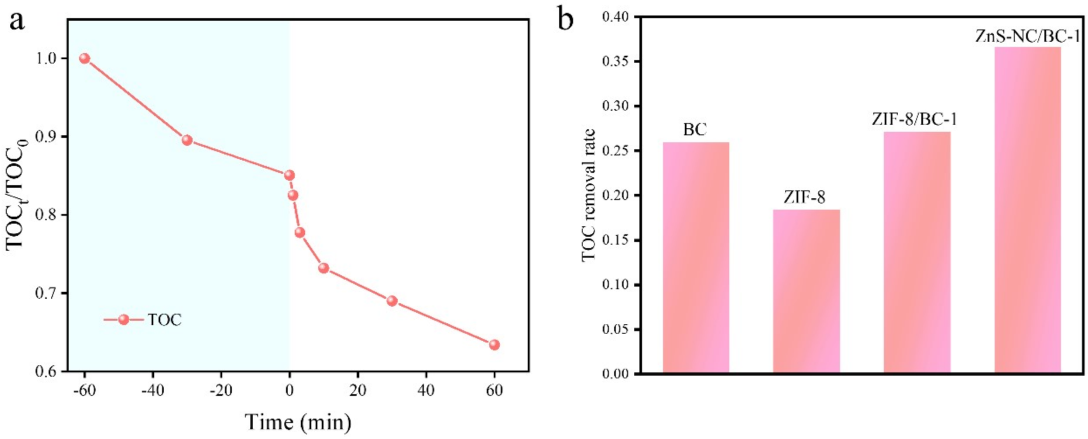

Fig. S6. (a) TOC removal in ZnS-NC/BC-1.0+PMS system. (b) Comparison of the mineralized TOC of different systems.

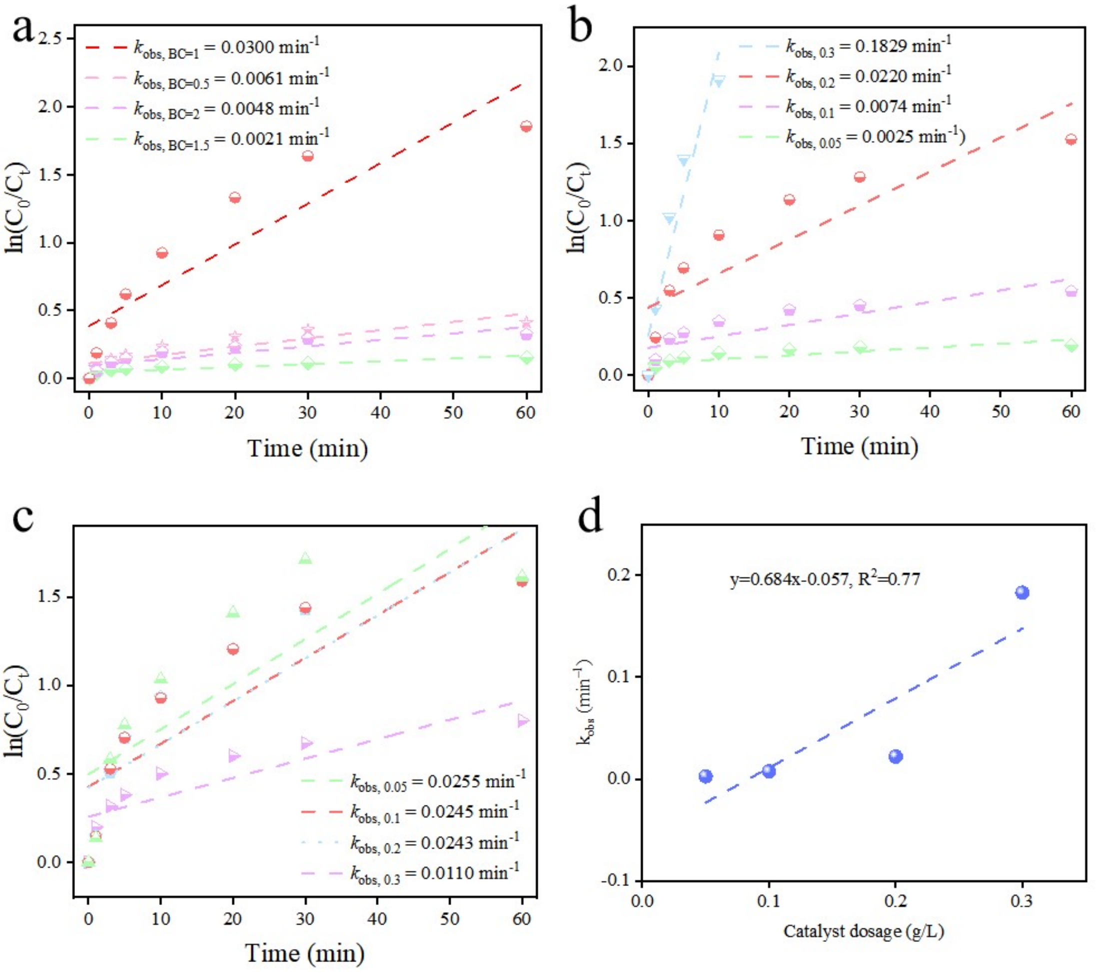

Fig. S7. Pseudo-first-order kinetic rate of 4-CP degradation under (a) different doping amount of BC, (b) different catalysts dosage and (c) PMS concentration. (d) The correlation between catalyst dosage and the reaction kinetic. Reaction conditions: [4-CP] = 10 mg/L, [catalyst] = 0.2 g/L, [PMS] = 0.1 g/L.

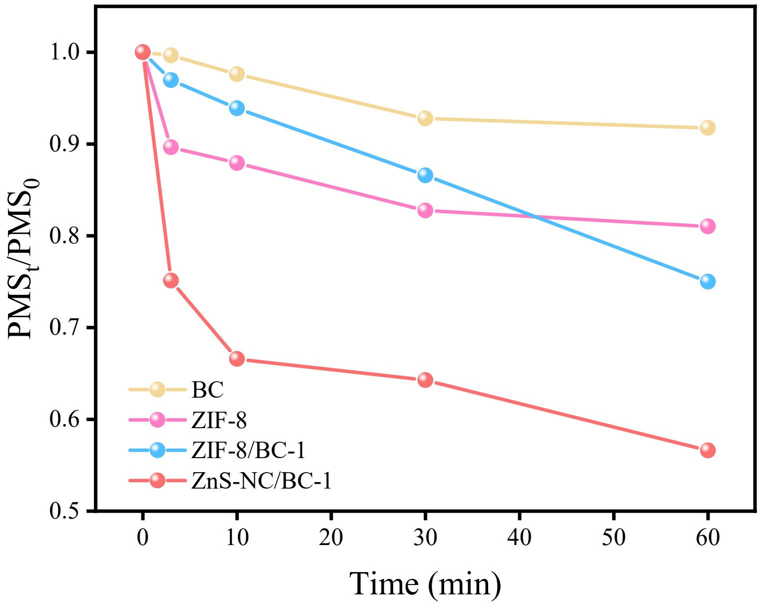

Fig. S8. PMS residual amount in different systems.

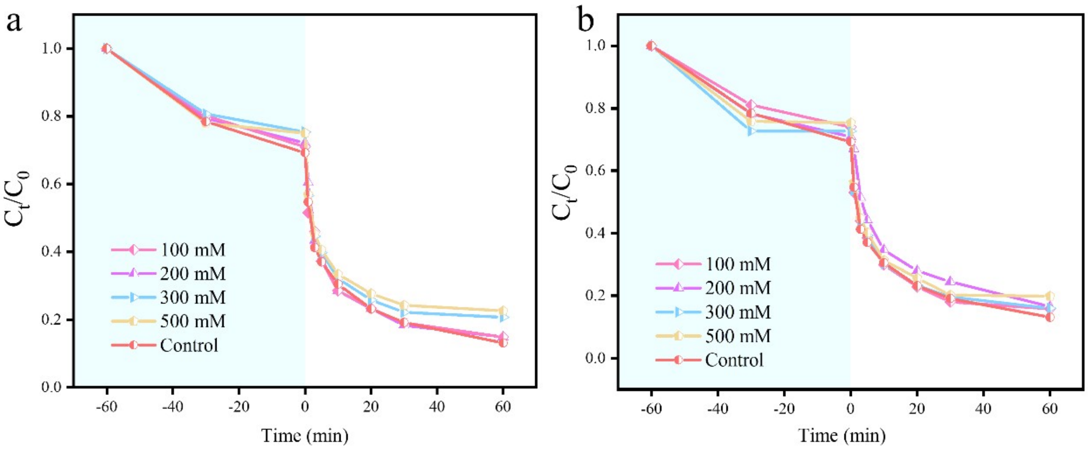

Fig. S9. Effect of different concentration of (a) MeOH and (b) TBA on 4-CP degradation.

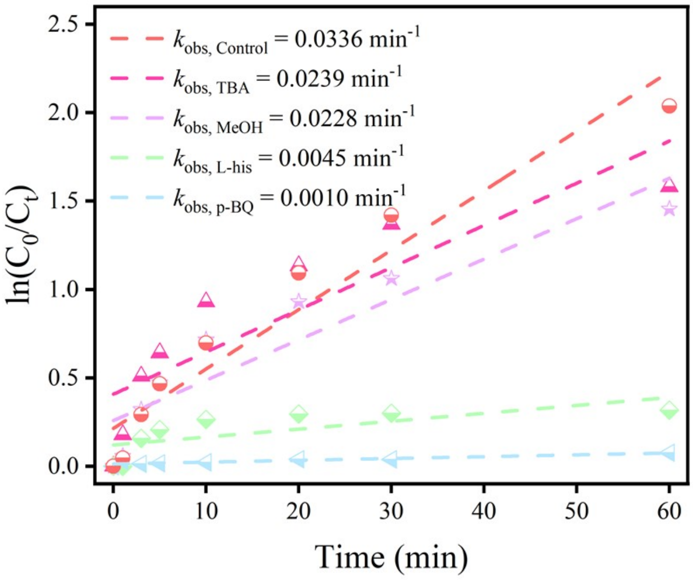

Figure S10. The reaction kinetic of quenching experiment.

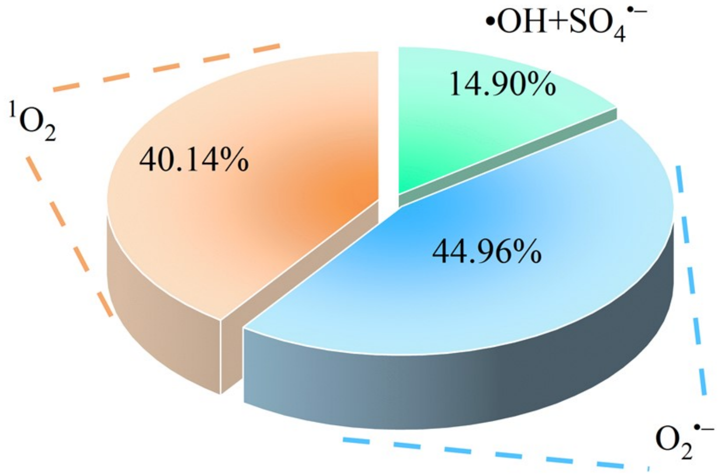

Figure S11. Proportion of active species for 4-CP removal.

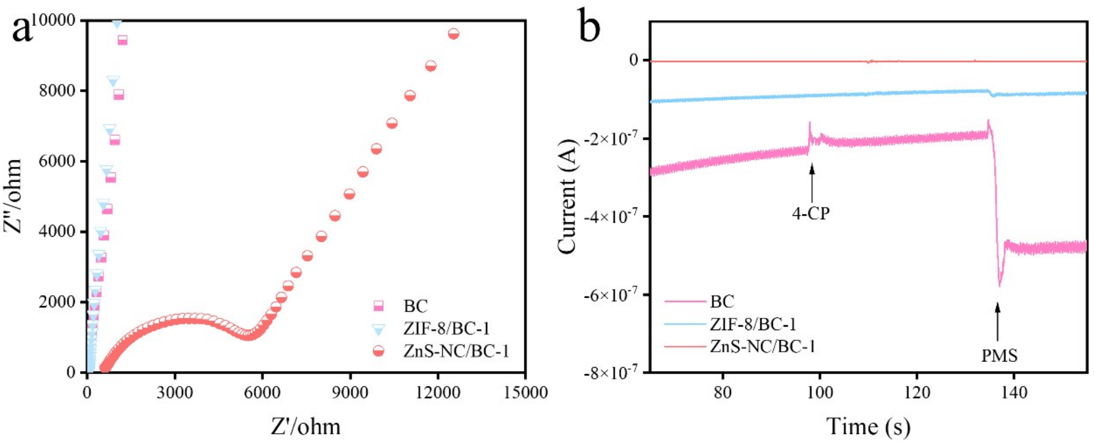

Fig. S12. EIS measurement (a) and i-t curves (b) for electro-system with BC, ZIF-8/BC-1, and ZnS-NC/BC-1 electrode.

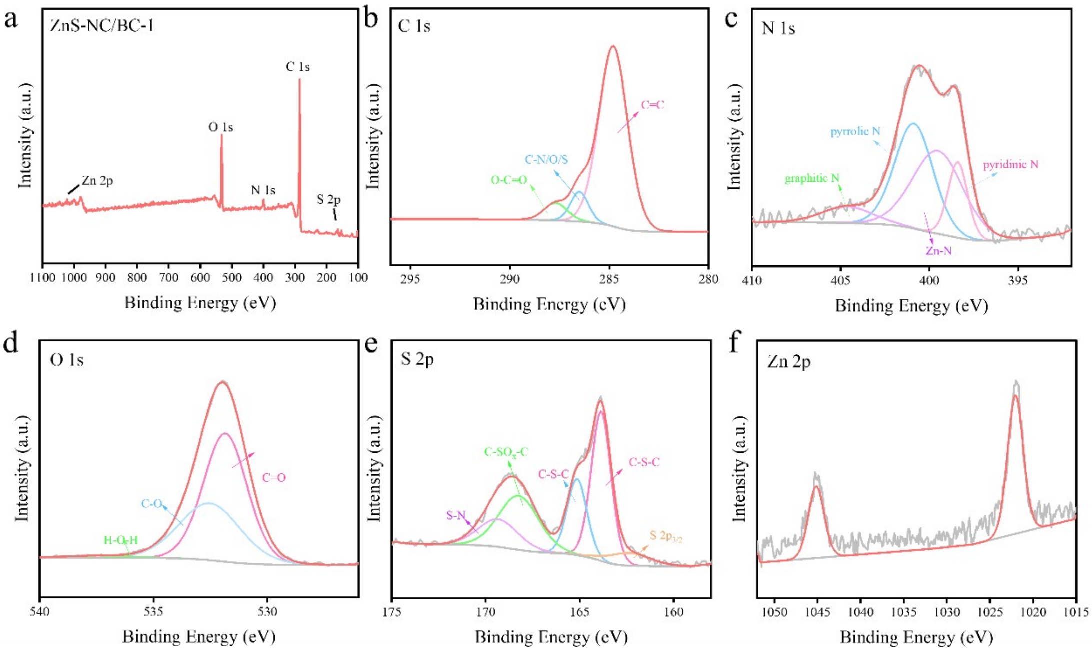

Fig. S13. (a) XPS survey spectra of ZnS-NC/BC-1 after reaction; (b-f) High-resolution XPS spectra of C 1s, N 1s, O 1s, S 2p, Zn 2p, respectively.

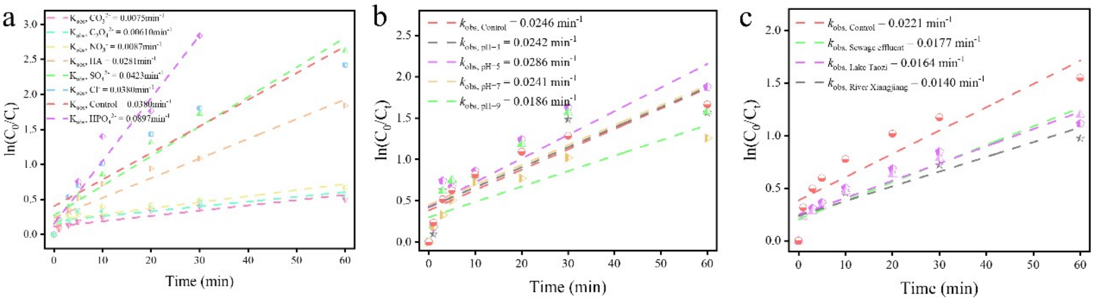

Fig. S14. The pseudo-first-order kinetic rate of the 4-CP under (a) anions and HA; (b) different pH; and (c) natural water and sewage effluent. Reaction conditions: [4-CP] = 10 mg/L, [catalyst] = 0.2 g/L, [PMS] = 0.1 g/L.

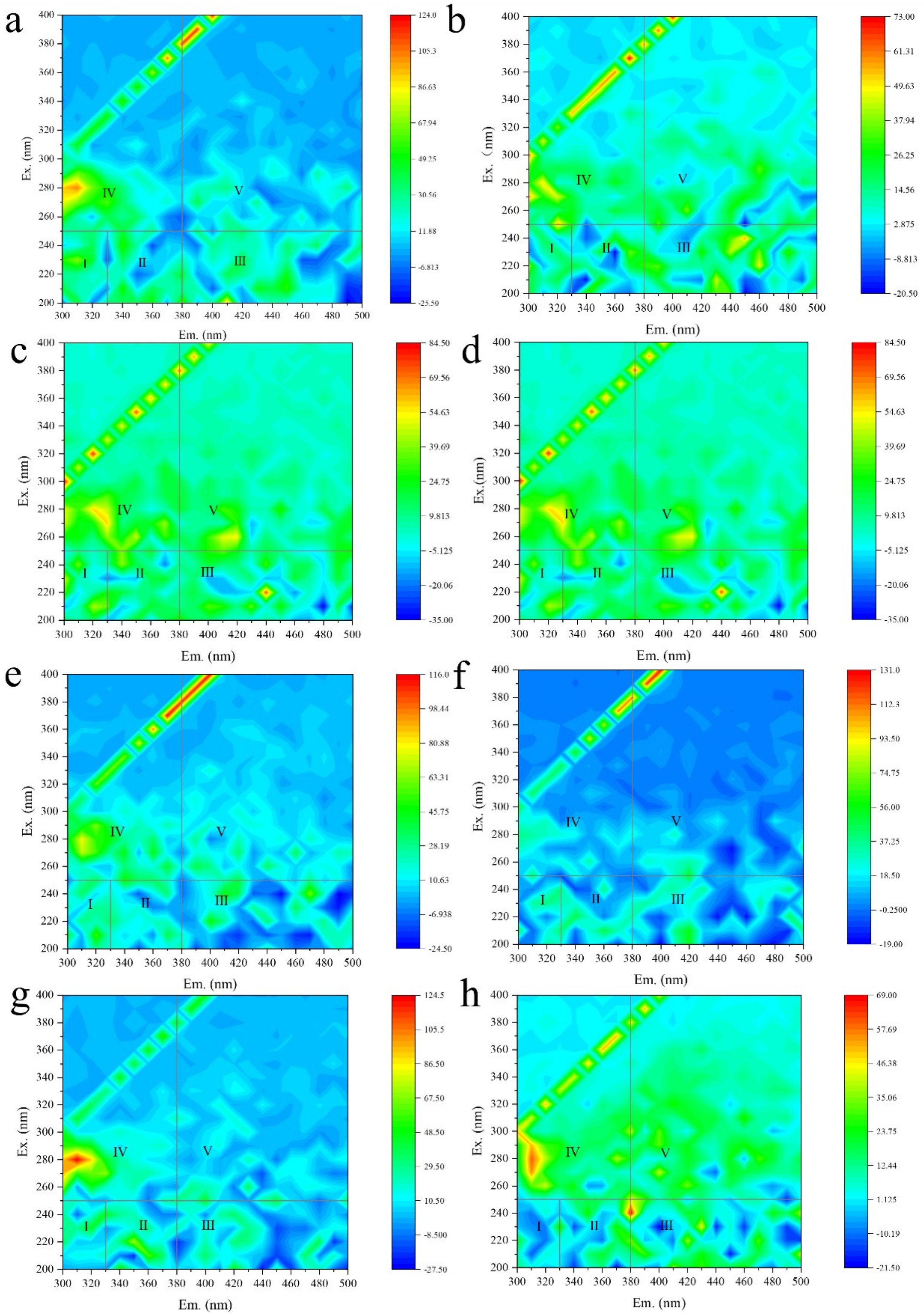

Fig. S15. EEM of the 4-CP solution before (0 min) and after degradation (60 min) in (a) and (b) ultrapure water, (c) and (d) Lake Taozi, (e) and (f) River Xiangjiang, (g) and (h) Sewage effluent water.

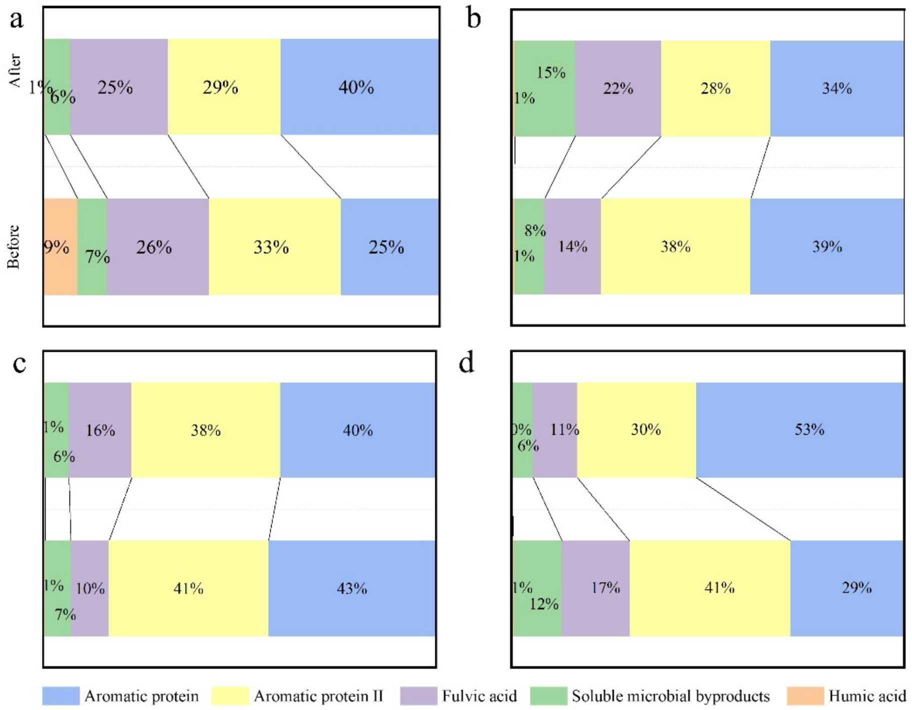

Fig. S16. Changes in solution composition before and after the reaction of (a) ultrapure water, (b) Lake Taozi, (c) River Xiangjiang and (d) Sewage effluent, respectively.

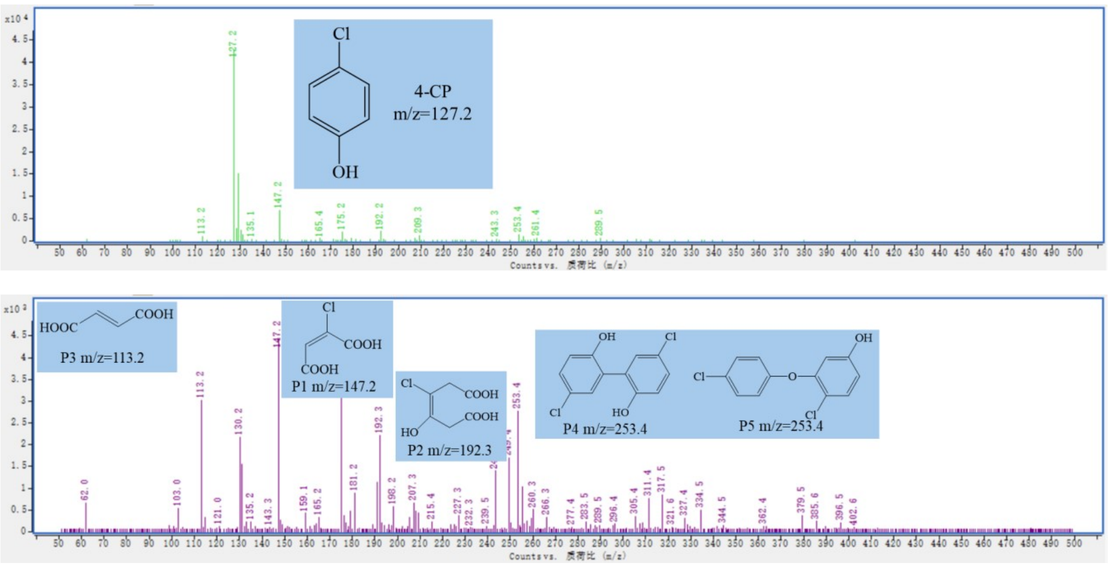

Fig. S17. Mass spectrogram of 4-CP degradation intermediates

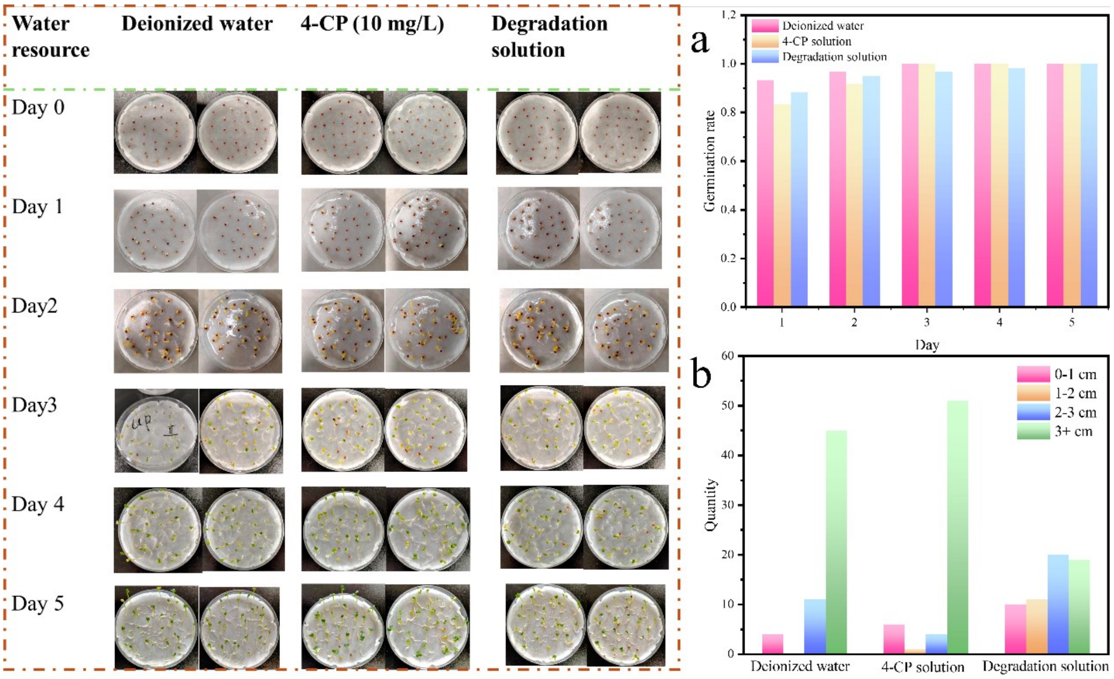

Fig. S18. Records of Pakchoi germination and growth. (a) Germination rate and (b) root length in day 5 of Pakchoi under deionized water, 4-CP solution and degradation solution cultivation conditions.

Table S1. The detailed gradient elution of LC-MS.

Time (min)	0.1% formic acid	MeOH	eluent rate (ml/min)	m/z	Mode
0	90%	10%	0.2	50-600	Negative
4	90%	10%	0.2		
14	10%	90%	0.2		
20	10%	90%	0.2		
21	90%	10%	0.2		
22	90%	10%	0.2		

Table S2. Specific surface area, pore volume and average pore size distribution of catalysts.

Catalysts	S_{BET} ($m^2 \cdot g^{-1}$)[a]	V_{total} ($cm^3 \cdot g^{-1}$)[b]	V_{mic} ($cm^3 \cdot g^{-1}$)[c]	D_{aver} (nm)[d]	$D_{meo, aver}$ (nm)[e]
BC	1.02	0.0033	0.0002	12.76	24.93
ZIF-8	838.70	0.3868	0.3553	1.84	3.39
ZIF-8/BC-1	364.01	0.1412	0.1346	1.55	5.42
ZnS-NC/BC-1	187.56	0.0924	0.0735	1.97	4.74
ZnS-NC/BC-1 before acid wash	83.468	0.0473	0.0301	2.34	4.71

[a] Specific surface area from multiple Brunauer-Emmett-Teller (BET) method.

[b] Single point adsorption total pore volume of pores less than 386.25 nm diameter at $P/P_0 = 0.9950$.

[c] t-Plot micropore volume.

[d] Adsorption average pore diameter (4V/A by BET).

[e] BJH adsorption average pore diameter (4V/A).

Table S3: The contents of different elements in different ZnS-NC/BC-1.

Element	ZnS-NC/BC-1 before acid wash	ZnS-NC/BC-1 after acid wash	ZnS-NC/BC-1 after cycling
C	74.04	77.76	73.69
N	5.79	6.15	5.98
O	15.03	13.65	17.39
S	2.58	2.11	2.87
Zn	2.55	0.33	0.07

Table S4. Percentage content of different forms of N and S in different ZnS-NC/BC-1.

Element	Different forms	ZnS-NC/BC-1 before acid wash	ZnS-NC/BC-1 after acid wash	ZnS-NC/BC-1 after cycling
N	Pyridinic N (at%)	21.8	51.94	5.39
	Zn-N (at%)	30.69	21.37	39.88
	Pyrrolic N (at%)	34.49	17.79	38.13
	Graphitic N (at%)	13.01	8.89	7.96
S	S $2p_{1/2}$ and S $2p_{3/2}$ (at%)	65.56	3.6	3.31
	C-S-C (at%)	23.67	42.67	55.9
	Oxidized S (at%)	5.39	26.85	20.39
	S-N (at%)	5.39	26.87	20.4

Table S5. The correlation analysis between k_{obs} and various factors based on Spearman correlation by IBM SPSS Statistics 26.

	Doping amount (g)	Catalyst dosage (g/L)	PAA doges (g/L)	k_{obs} (min^{-1})
Doping amount (g)	1			
Catalyst dosage (g/L)	0.036	1		
PAA concentration (g/L)	-0.036	0.036	1	
k_{obs} (min^{-1})	-0.349	0.569*	-0.119	1

*. At the 0.05 level (double tailed), the correlation is significant.

Table S6. Basic physical and chemical indicators of natural water and sewage water.

Water matrix Indicator	River Xiangjiang	Lake Taozi	Sewage effluent
pH	7.08	7.00	6.80
Total hardness	31.51 mg/L	28.61 mg/L	40.13 mg/L
Total organic carbon	1.049 mg/L	2.595 mg/L	8.131 mg/L
COD_{Cr}	5 mg/L	13 mg/L	41 mg/L
Mg	<0.000 μg/L	<0.000 μg/L	<0.000 μg/L
K	<0.000 μg/L	<0.000 μg/L	<0.000 μg/L
Cr	2.681 μg/L	0.014 μg/L	<0.000 μg/L
Mn	<0.000 μg/L	<0.000 μg/L	<0.000 μg/L
Fe	<0.000 μg/L	<0.000 μg/L	<0.000 μg/L
Co	0.295 μg/L	0.065 μg/L	0.004 μg/L
Ni	<0.000 μg/L	1.510 μg/L	4.332 μg/L
Cu	0.933 μg/L	0.221 μg/L	0.025 μg/L
Zn	14.611 μg/L	<0.000 μg/L	<0.000 μg/L
Ga	<0.000 μg/L	0.120 μg/L	0.016 μg/L
As	12.608 μg/L	0.005 μg/L	<0.000 μg/L
Cd	<0.000 μg/L	<0.000 μg/L	<0.000 μg/L
Tl	0.014 μg/L	0.234 μg/L	0.116 μg/L
Pb	<0.000 μg/L	<0.000 μg/L	<0.000 μg/L

Table S7. The main degradation intermediates of 4-CP.

Compounds	m/z	Chemical formula	Structure
4-CP	127.2	C_6H_5OCl	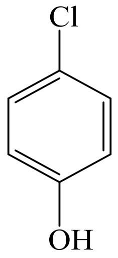
P1	147.2	$C_4H_3O_4Cl$	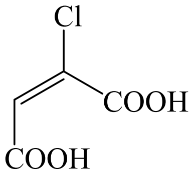
P2	192.3	$C_6H_7O_5Cl$	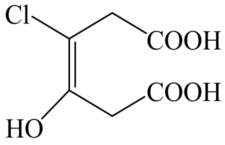
P3	113.2	$C_{12}H_9O_2Cl$	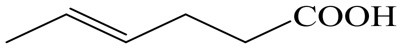
P4	253.4	$C_4H_5O_2$	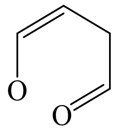
P5	253.4	$C_{12}H_8O_2Cl_2$